An effective strategy for improving charge separation efficiency and photocatalytic degradation performance by facilely synthesized oxidative TiO₂ catalyst

Yongqi Qin[*a,b],‡ Liqiang Deng [a,b],‡ Shaodong Wei [a,b], Hui Bai [d], Wenqiang Gao [a,b,c],

Weizhou Jiao[* c] , Tanlai Yu[*a,b]

[a] Lvliang Key Laboratory of Comprehensive Utilization of Organic Waste Resources, Department of Chemistry and Chemical Engineering, Lvliang University, Lvliang 033001, Shanxi, China

[b] Lvliang Key Laboratory of Optical and Electronic Materials and Devices, Lvliang University, Lvliang 033001, Shanxi, China

[c] Shanxi Province Key Laboratory of Higee-Oriented Chemical Engineering, North University of China, Taiyuan 030051, Shanxi, China

[d] Key Laboratory of Coal Science and Technology of Ministry of Education and Shanxi Province, Taiyuan University of Technology, Taiyuan 030024, Shanxi, China

* Corresponding authors: Yongqi Qin, E-mail: qinyq2003@163.com; Weizhou Jiao, E-mail: jwz0306@126.com; Tanlai Yu: E-mail: yutanlai1212@126.com/ tlyu@llu.edu.cn.

Materials

Anatase titanium dioxide (≥99%) was purchased from Shandong Pingju Biological Technology Co. LTD. Potassium permanganate (KMnO₄) was obtained from Taihua Chemical and Agrochemical Factory. Benzoquinone and methyl orange were purchased from Tianjin Guangfu Technology Development Co. LTD. Tert-butanol, 5,5-dimethyl-1-pyrrolidine-N-oxide (DMPO), sodium oxalate, and hydrochloric acid were purchased from Aberdeen Technology Co. LTD.

Table S1 Kinetics study results of Methyl Orange (MO) degradation by oxidative TiO₂ samples.

Photocatalysts	Light source	Reaction temperature	KMnO₄ adding	Pseudo-first order kinetic model equation: $\ln(A_0/A_t) = kt$	
				k (min^{-1})	R^2
Oxidative TiO₂ (a)	Xe lamp	80°C	0.5%wt	0.0120	0.99731
Oxidative TiO₂ (b)	Xe lamp	80°C	1.0%wt	0.00912	0.99841
Oxidative TiO₂ (c)	Xe lamp	80°C	2.0%wt	0.01274	0.99839
Oxidative TiO₂ (d)	Xe lamp	80°C	2.5%wt	0.01222	0.99866
Oxidative TiO₂ (e)	Xe lamp	80°C	3.0%wt	0.01114	0.9984
Oxidative TiO₂ (f)	Xe lamp	80°C	3.5%wt	0.01352	0.99327
Oxidative TiO₂ (g)	Xe lamp	80°C	4.0%wt	0.01566	0.99829
Oxidative TiO₂ (h)	Xe lamp	25°C	4.0%wt	0.01431	0.99697
Oxidative TiO₂ (i)	Xe lamp	150°C	4.0%wt	0.01321	0.99468
Oxidative TiO₂ (j)	Xe lamp	200°C	4.0%wt	0.00967	0.98811

[a] where A_0 is the initial absorbance of MO solution; A_t is the absorbance of MO solution after time (t) of degradation; Parameters were fixed at: $A_0 = 1.084$, pH = 6.0 and [catalyst]$_0$ = 0.2g/L.

Table S2 Structural Parameters of oxidative TiO_2 and pristine TiO_2.

Sample	Crystallite Size D (nm)	dislocation density (δ) (line/m^2) ($\times10^{16}$)	microstrain (ε) ($\times10^{-2}$)
Pristine TiO_2	5.40	3.42	6.38
Oxidative TiO_2	5.67	3.12	6.04

[a] Scherrer Formular: where D = (0.89 × λ) / (β ×Cosθ) where, λ = 1.5406 nm.

[b] Williamson and Smallman equation: $\delta = \frac{n}{D^2}$.

[c] $\varepsilon = \frac{\beta cos\theta}{4}$.

Table S3 Interplanar spacing of oxidative TiO_2 and pristine TiO_2.

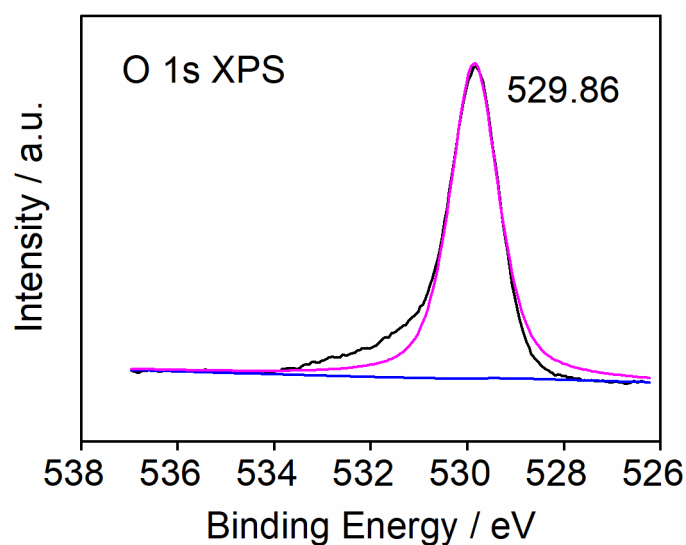| (hkl)planes	Pristine TiO_2		Oxidative TiO_2	
	Peak position (2θ)	Interplanar Spacing (d) / Å	Peak position (2θ)	Interplanar Spacing (d) / Å
101	25.40	3.5033	25.32	3.5140
103	37.08	2.4226	36.99	2.4280
004	37.84	2.3757	37.83	2.3762
112	38.56	2.3331	38.45	2.3392
200	48.16	1.8879	48.08	1.8908
105	53.99	1.6971	53.94	1.6985
211	55.20	1.6627	55.11	1.6651
116	68.84	1.3627	68.83	1.3630
220	70.34	1.3373	70.36	1.3369
215	75.10	1.2639	75.12	1.2639
301	76.07	1.2502	76.11	1.2497

[a] Bragg's equation was used to estimate the interplanar distances (d). $n\lambda = 2dsin\theta$.

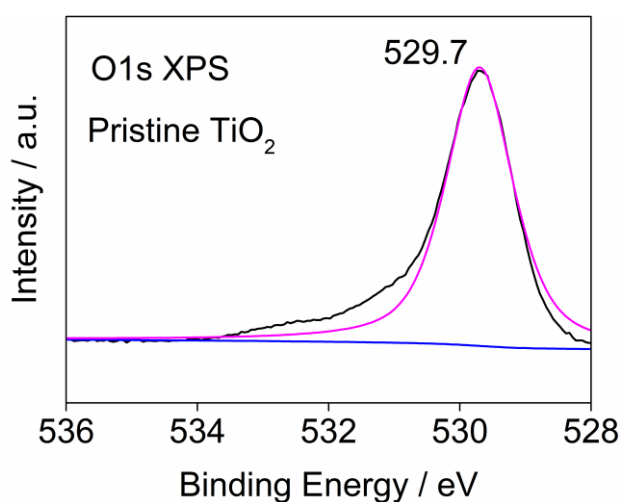**Table S4** Lattice parameters and cell volume of oxidative TiO$_2$ and pristine TiO$_2$.

sample	a (Å)	c (Å)	Volume (Å^3)
Oxidative TiO$_2$	3.7815	9.5121	136.02
Pristine TiO$_2$	3.7759	9.3906	133.89

[a] Where $\frac{1}{d^2} = \frac{h^2+k^2}{a^2} + \frac{l^2}{c^2}$ (Tetragonal phase).

[b] $V = a^2c$.

Fig. S1 High-resolution XPS spectra of O 1s for oxidative TiO$_2$ synthesized at 200°C.

Fig. S2 High-resolution XPS spectra of O 1s for pristine TiO$_2$.
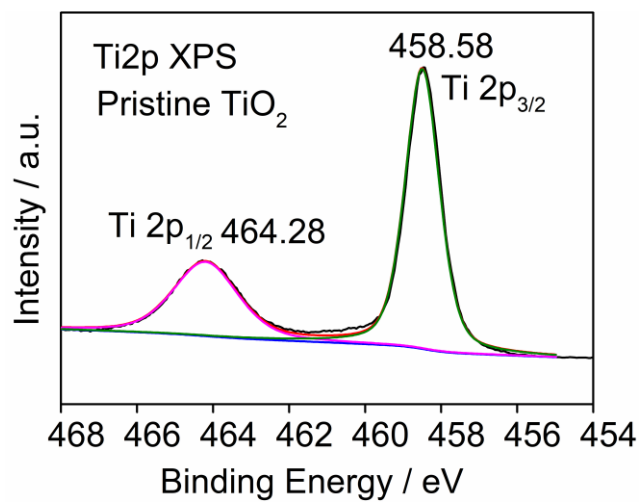
Fig. S3 High-resolution XPS spectra of Ti 2p for pristine TiO$_2$.
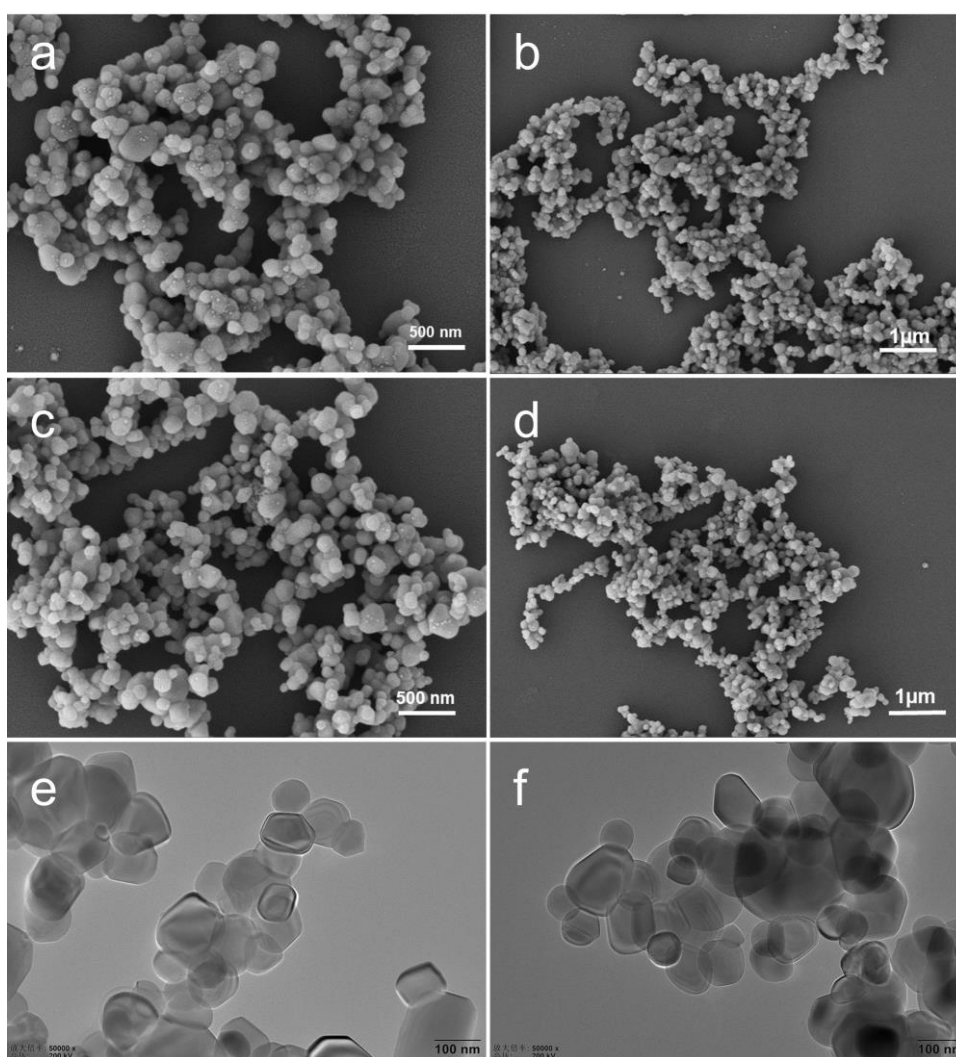
Fig. S4 SEM images of oxidative TiO$_2$ (a, b) and pristine TiO$_2$ (c,d). TEM images of oxidative TiO$_2$ (e) and pristine TiO$_2$ (f).
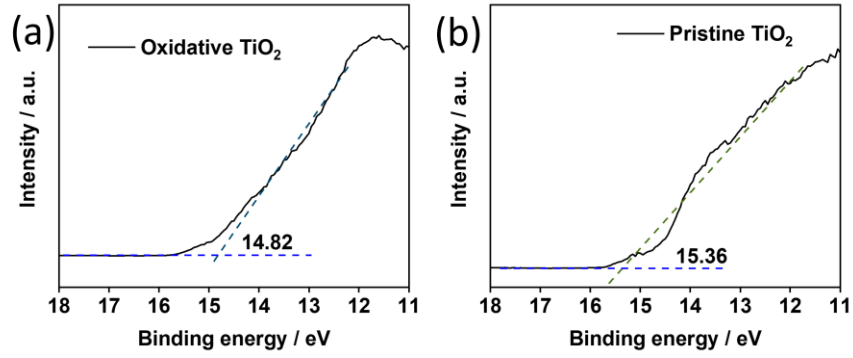
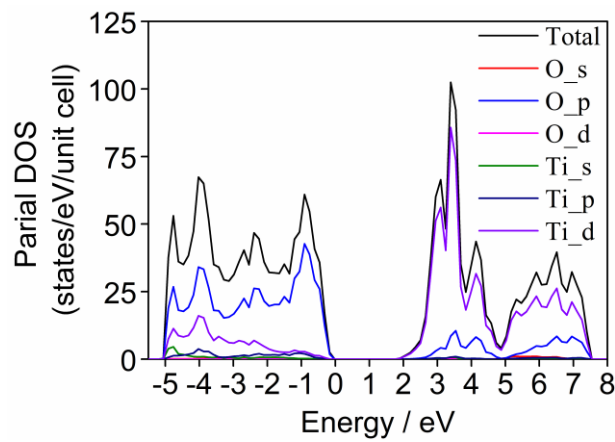**Fig. S5** UPS spectra of oxidative TiO$_2$ (a) and pristine TiO$_2$ (b).
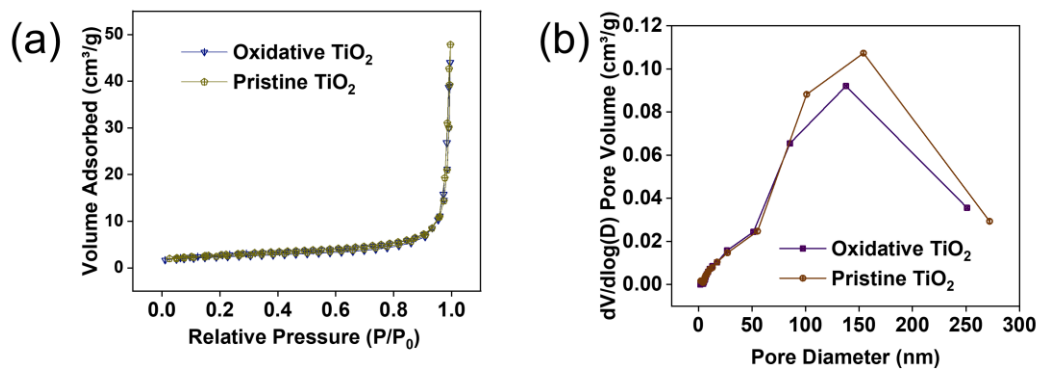

Fig. S6 Calculated DOS of pristine TiO$_2$.

Fig. S7 N$_2$ adsorption-desorption isotherms(a) and BJH pore size distribution curves (b).
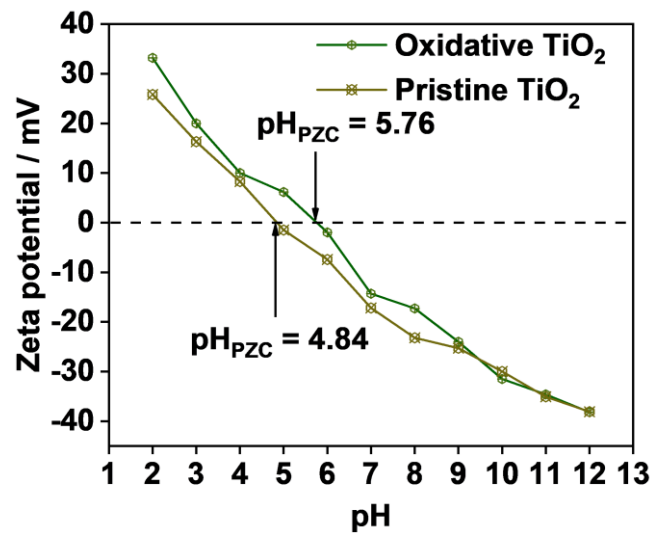
Fig. S8 Zeta potential of oxidative TiO_2 and pristine TiO_2.
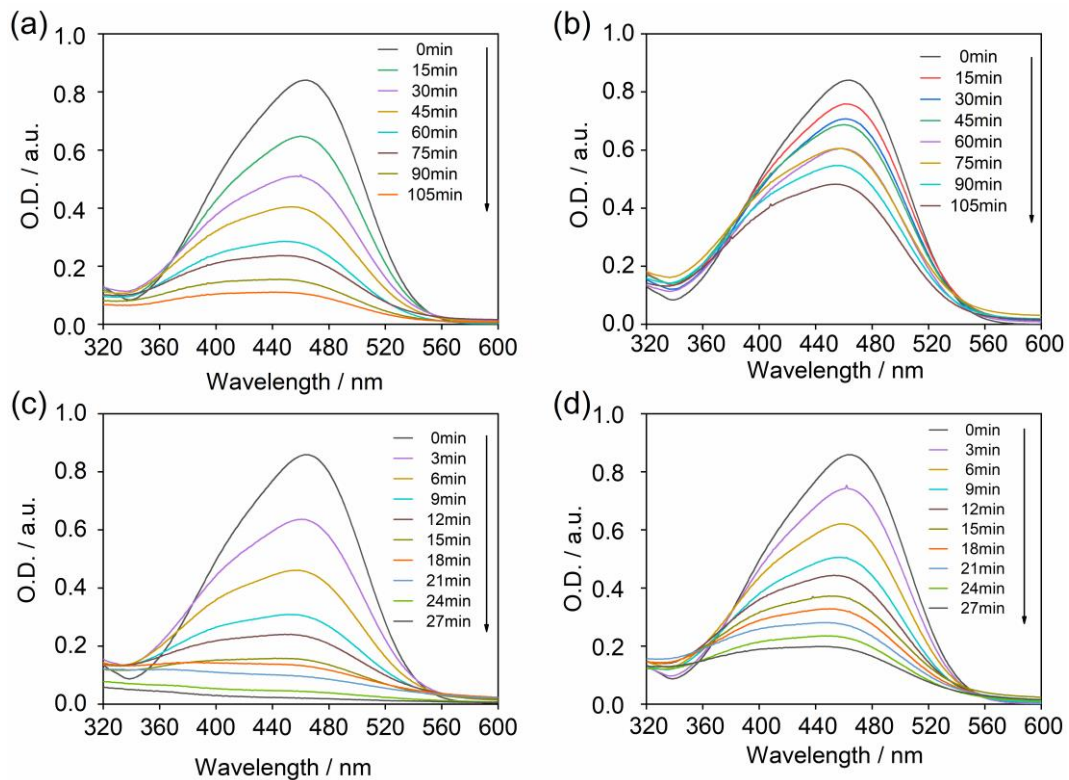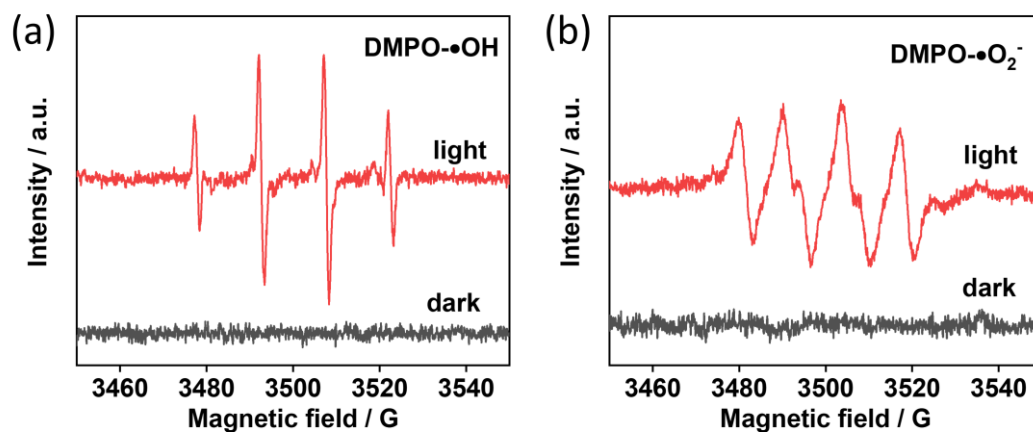

Fig. S9 UV-vis spectra of MO solution at different time under simulated sunlight irradiation using (a) oxidative TiO_2 and (b) pristine TiO_2. UV-vis spectra of MO solution at different time under UV light using (c) oxidative TiO_2 and (d) pristine TiO_2.

Fig. S10 ESR spectra of pristine TiO_2 under Xe lamp irradiation and in the dark: (a) DMPO-•OH and (b) DMPO-• O_2^-.